Journal of Education for Pure Science- University of Thi-Qar
Vol.13, No.2 (June., 2023)
Website: jceps.utq.edu.iq Email: jceps@eps.utq.edu.iq

DOI: http://doi.org/10.32792/utq.jceps.10.01.01

# Automated Approach for Depression Recognition Using Fast Fourier Transform Based EEG Signals

**Hadeer Mohammed[1], Mohammed Abdalhadi Diykh[1]**

Msc21co1@utq.edu.iq mohammed.diykh@utq.edu.iq;

[1]University of Thi-Qar, College of Education for Pure Science, Computer Science, Iraq

Corresponding email:;

**Received 16/4/2023, Accepted 11/5/2023, Published 11/6/2023**



**Abstract:**

Major Depressive Disorder (MDD) is the primary cause of impairment and one of the primary reasons for suicide. It is a serious ailment that millions of people are currently suffering from it. Any decline in brain function during MDD or depression is evident in the Electroencephalogram (EEG) signals. In this study, a Fast Fourier transform (FFT) method-based automated framework for depression recognition is proposed. Firstly, EEG signals from each channel are divided using FFT into five frequency bands (α, β, γ, δ and θ). Next, nonlinear features are extracted from each band, including approximation entropy, dispersion entropy, Shannon entropy, and Second Order Different Plot (SODP). The Mann-Whitney U test is used to get rid of undesirable features that could harm learners' performance. The selected features are passed to the least square support vector machine (LS-SVM) for comparison with other classifiers, including the support vector machine (SVM), k-nearest Neighbour (KNN), and decision tree (DT). The performance of the suggested model is assessed using K-fold cross-validation. A publicly accessible dataset was used to model our investigations. The results showed that the reduction of features can lead to high accuracy, where the highest accuracy obtained was 0.96%, it was using the LS-SVM classifier, with Shannon Entropy and SODP features only from the delta and gamma bands.

**Keywords:** MDD, EEG, LS-SVM, Entropy, SODP, FFT band filter

## Introduction

Anger, sorrow, and anxiety are all symptoms of major depressive disorder (MDD), a significant mood illness [1] [2] [3]. It can result in emotional, physical, and cognitive problems that raise the risk of Alzheimer's disease and suicide, with the global suicide rate due to depression reaching 3.7% and accounting for over 850,000 suicidal deaths worldwide [4]. The World Health Organization estimates that depression affects more than 350 million people worldwide between the ages of 20 and 70, and that it will likely overtake all other diseases by the year 2030 [5][6][7].

The primary causes of depression may be hereditary or environmental, including stress, worry, and anxiety. In addition, a number of recent researchers found that the COVID-19 pandemic increased the incidence of depression in people for a variety of reasons, such as home quarantine, unemployment, and social isolation [8] [9]. For appropriate treatment to be determined and to prevent the disease from worsening, early diagnosis of depression is essential.

The traditional approaches to a depression diagnosis, such as clinical trials and questionnaires, receive many criticisms as they are subjective in their nature [10], and many depressed individuals may not receive an accurate diagnosis [11]. Therefore, to lessen the subjectivity of MDD diagnosis, it is vital to find and improve MDD diagnosis methodologies based on biological indications. Numerous studies have been conducted to determine whether a person is depressed based on their interaction way on social media [10], electroencephalogram (EEG) signals [11] [12] [13], speech [14], and facial expressions [15]. The electroencephalogram (EEG) signal, which represents brain activity, is a biological indicator that can be used to objectively and accurately diagnose mental diseases. It can offer high temporal resolution data on the bioelectrical activity of the brain, and any changes in brain function or mental state may be reflected in these signals. However, due to their complexity, non-linearity, and non-stationarity, manual interpretation of EEG data is challenging [11]. As a result of the development of machine learning and computer technology, numerous researchers are examining EEG-based machine learning techniques to create computer-aided diagnostic (CAD) systems for facilitating the identification of neurological disorders.

Acharya et al. [16] by carefully combining nonlinear properties such as fractal dimension, sample entropy, maximum Lyapunov exponent, Hurst's exponent, detrended fluctuation analysis, recurrence quantification analysis, and higher order spectra; they presented a novel Depression Diagnosis Index (DDI). After that the SVM classifier receives these characteristics in order according to their rank using the t-value. Li et al. [17] employed a CNN to categorize people with mild depression and healthy controls by converting time series of EEG signals into images by computing the functional connectivity matrices. Mumtaz et al. [2] proposed a method to create a feature matrix using wavelet transform (WT) analysis and time-frequency decomposition of EEG data, the features were also used based on their accuracy in classifying 33 patients and 30 healthy subjects. Bachmann et al. [18] looked into several EEG features to spot depressed subjects. Different features were extracted: alpha power variability, relative gamma power, Higuchi's fractal dimension, detrended fluctuation analysis, and Lempel-Ziv complexity. EEG features were divided into control and depressed patients using a logistic regression approach. Sharma et al [19] created a wavelet filter bank-based computer-aided depression diagnosis model. Seven sub-bands were used by breaking down EEG signals. To categorize EEG characteristics, a LS-SVM was used. Saeedi Maryam et al. [20] proposed a model-based wavelet approach combined with machine learning models to diagnose depression. EEG signals were divided into five frequency bands, delta, theta, alpha, beta, and gamma using a wavelet process. Each wavelet band was used to extract a set of nonlinear features, and the most important features were then chosen using a genetic algorithm. For EEG classification, a set of classifiers including KNN, SVM, and multilayer perceptron were used. Mahato Shalini et al. [21] identified the most potent features using a multi cluster feature selection methodology. The classification of depressed participants was done using a variety of classifiers. Akbari Hesam et al.

[22] suggested a method using the reconstructed phase space (RPS) to identify depressions in EEG signals. A total of 34 geometrical features were extracted from each EEG recording using RPS. They demonstrated that, in comparison to the left hemisphere, the right hemisphere's EEG patterns substantially mirrored depression.
The fact that a combination of entropy and second-order difference plot (SODP) is not examined for MDD diagnosis is one of the problems with the earlier studies. To solve this problem, a suggested model that combines two different types of characteristics from five different EEG signal bands with an analysis utilizing an FFT band filter intends to diagnose MDD.

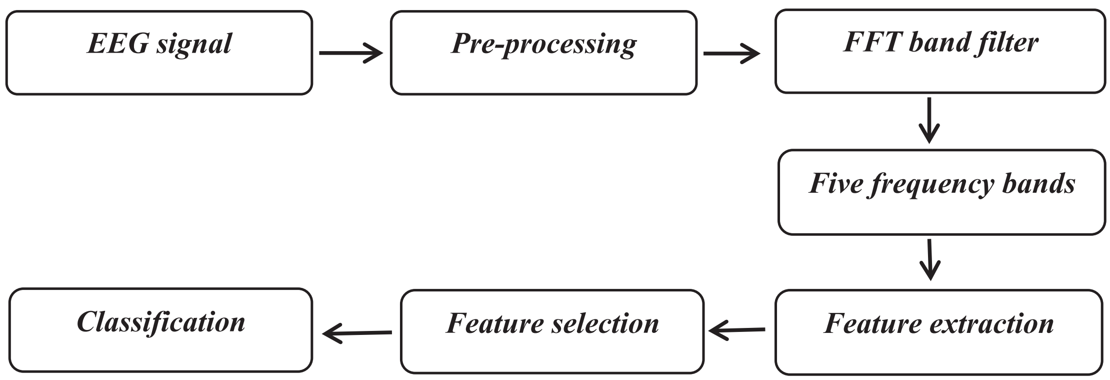


**Figure 1:** Flow diagram of the proposed approach

**Research methodology**

The purpose of this study is to create an efficient method of classifying depression using EEG signals. The signal is analysed into five frequency bands (alpha, beta, delta, theta, and gamma) by passing it to the FFT band filters. Fig. 1 shows the block diagram of the proposed model, which mainly consists of the pre-processing stage, analysis of EEG signals into five frequency bands, feature extraction, feature selection and classification.

**Materials and methods**

**1. EEG signal recording and Pre-processing**

Using a publicly available data set published by Mumtaz et al. [2], the suggested method for diagnosing depression based on EEG signals was investigated. The outpatients at Hospital Universiti Sains Malaysia participated in this study (HUSM). This dataset was collected from 30 healthy (9 females + 21 males, with (38.3 + 15.6) mean age) and 34 MDD patients (17 females + 17 males,(40.3 + 12.9) as mean age). Each participant completed a consent form for participation and was informed of the procedure for gathering experimental data. The experimental design was accepted by HUSM's ethics committee [2].
The MDD and HC patients' resting-state EEG signals were recorded, and a 19-channel EEG cap was used. The linked-ear (LE) reference [23]. An extra 50 Hz notch filter was employed to filter out power line noise after the signals were recorded at 256 HZ and filtered using bandpass filtered from 0.5 Hz to 70 Hz.

## 2. EEG Decomposition

Electroencephalography (EEG) which measures the electrical activity of the brain often used in the diagnosis of various disorders, including depression [25]. Using an FFT band filter is one way to break down an EEG signal into different frequency bands; the signal must first be subjected to an FFT to transform it from the time domain to the frequency domain. After that, you can isolate particular frequency bands by applying a filter function to the frequency domain of the signal [26].

For instance, we can choose to focus on the delta (0.5−3Hz) or theta (4−7Hz) frequency bands. This can achieve by reducing any frequency components outside of the delta or theta bands to zero using a band-pass filter on the signal's frequency domain. The filtered signal can then be converted back to the time domain using an inverse FFT (IFFT), yielding a signal that only consists of the delta or theta frequency range. The original EEG signal can be broken down into its constituent frequency components by repeating this procedure for other frequency bands.

In this study, the EEG signal was divided into five different frequency components: δ (delta), θ (theta), α (alpha), β (beta), and γ (gamma). These five frequency bands are depicted in Fig. 2 for both healthy controls and MDD patients, which display from the lower frequency band to the higher frequency band.

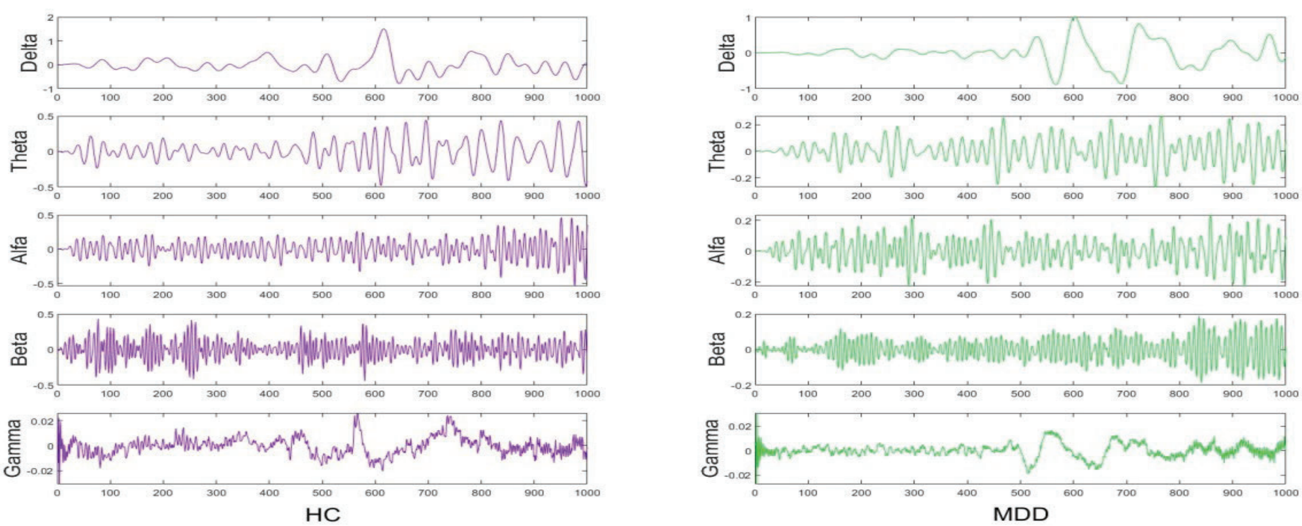


**Figure 2:** The five frequency bands of healthy and depressive EEG signals.

Details of these bands with their amplitudes and frequencies in the healthy state are shown in Table 1. [27] [28]

**Table 1:** The five frequency bands of EEG signal.

| *Bands* | *Frequencies range* | *Amplitude* | *Human mental stages* |
|---|---|---|---|
| delta | 0.5Hz − 3Hz | 20 − 200 | Deep sleep |
| theta | 4Hz − 7Hz | 2 − 100 | sleeping |
| alpha | 8Hz − 12Hz | 20 − 60 | Awake and resting |
| beta | 13Hz − 30Hz | 2 − 20 | Awake with mental activity |
| gamma | 30Hz − 100Hz | 5 − 10 | Higher mental activity |

**Fast Fourier transforms (FFT)**

The fast Fourier transform is an effective method for computing the discrete Fourier transform (DFT), which separates signals into components with various frequencies. It is able to extract a signal's phase spectrum, amplitude, and angle characteristics. It is one of the most widely used techniques for converting data from a time domain to a frequency domain [29]. Make $x_0, \ldots, x_{L-1}$ be complex numbers. The DFT is defined by the equation:

$$X_v = \sum_{m=0}^{L-1} x_m \, . \, e^{-i2\pi vm/L} \qquad (1)$$

Where $e^{i2\pi/L}$, is a primitive Lth root of 1.

FFT is a divide-and-conquer approach that reduces processing time by recursively splitting the DFT into smaller DFTs. where Cooley and Tukey shown that if we keep breaking the problem down into smaller ones, we can calculate DFT Eq. (1), more quickly. After splitting the entire series into two sections, odd and even number parts:

$$X_v = \sum_{n=0}^{L/2-1} x_{2n} \, . \, e^{-i2\pi v(2n)/L} + \sum_{n=0}^{L/2-1} x_{2n+1} \, . \, e^{-i2\pi v(2n+1)/L} \qquad (2)$$

$$X_v = \sum_{n=0}^{L/2-1} x_{2n} \, . \, e^{-i2\pi vn/(L/2)} + e^{-i2\pi v/L} \sum_{n=0}^{L/2-1} x_{2n+1} \, . \, e^{-i2\pi vn/(L/2)} \qquad (3)$$

The two parts in the equation above that have half of size only $(L/2)$ are two smaller DFTs. In each part the $0 \leq n \leq L/2$, but $0 \leq k \leq L$ As a result, we can observe that the DFT's symmetry features will lead half of each part's values to be the same. As a result, we just need to calculate half the values in each part. We can proceed and split each term into halves with even and odd values up until the final two digits, at which point the calculation will be uncomplicated [30].

The complexity of the DFT is successfully decreased from $O(L^2)$ to $O(L\,log(L))$, where the size of the data is represented by n. For data with big N, this decrease in computation time is very noteworthy. As a result, FFT is frequently employed in signal processing and has a wide range of applications, including digital filtering and spectral analysis [31].

## 3. Feature extractions

By taking into account only certain features that distinguish between normal and abnormal signals, the feature extraction stage reduces the original signal complexity. Due to the size of the EEG data, feature extraction transforms the complicated EEG signal into a smaller feature sample model.

The features that were extracted from each frequency band are described below.

### 3.1 Approximate Entropy (ApEn)

ApEn is a metric for measuring correlation or regularity; low values signify a system that is highly predictable, and regular, with manifests repeating patterns across the series, whereas high values suggest independence between the data, a lack of repeating patterns, and randomness. To put it another way, systems with larger random probabilities also have higher entropies [32].

### 3.2 Shannon Entropy

Shannon entropy is the average amount of "knowledge", or "uncertainty" associated with a random variable's potential outcomes [33]. A random variable $X's$ Shannon entropy can be expressed in terms of Eq. (4), where $P_i$ is defined in terms of Eq. (5), with $x_i$ signifying the $i^{th}$ possible value of $X$ out of $n$ symbols and $P_i$ denoting the possibility of $X = x_i$ [33].

$$H(X) = H(P_1, \ldots, p_n) = -\sum_{i=1}^{n} P_i \log_2 P_i \tag{4}$$

$$P_i \text{ defined as: } \quad P_i = P_r(X = x_i) \tag{5}$$

### 3.3 Dispersion Entropy (DisEn)

DisEn calculates a time series' complexity or irregularity [34]. It is produced by mixing symbolic dynamics with Shannon entropy, resulting in an algorithm that can quickly determine the degree of irregularity of the analysed signal segments while maintaining high discriminating power [35].

$$\mathrm{DispEn}(m, c) = -\sum_{i=1}^{c^m} p[\, y_m(i)] \log(p[\, y_m(i)]) \tag{6}$$

$$y_m(i) \; = \; [z^c(i), z^c(i+1), z^c(i+2), \ldots, z^c(i+m-1) \qquad (7$$

### 3.4 Second Order Different Plot (SODP)

SODP is a graphical tool that derives from chaos theory, and is used to examine how much variability there is in a time series. An essential characteristic of complex nonlinear systems that can be used to categorize them is the level of variability or chaos [36], [37]. The SODP plots consecutive rates $A(n)$ and $B(n)$ against one another for time series $a(n)$ of length $N$. These rates are specified as follows [38]:

$$A(n) \; = \; a(n+1) - a(n) \tag{8}$$

$$B(n) = \; a(n+2) - \; a(n+1) \tag{9}$$

## 4. Feature selection

Feature selection is the process of deciding a subset of pertinent features that will be used to build the model. By simplifying the model and getting rid of noise and useless data, feature selection aims to increase the model's interpretability and forecast accuracy. In this study, we evaluated the importance of each attribute using statistical techniques. The features with the highest values are kept. Mann-Whitney U-test is the measurement employed.

### Mann-Whitney U test

It is a nonparametric statistical test that is used to detect whether the medians of two groups differ significantly from one another. To test whether the medians of the two groups are significantly different, it ranks the values in each group and compares the ranks. Large disparities between the medians of the two populations are shown by low p-values. For each group, the following mathematical definitions of the Mann-Whitney U statistics are given:

$$Ux = mxmy + \left((mx(mx + 1))/2\right) - Kx \quad (10)$$
$$Uy = mxmy + \left((my(my + 1))/2\right) - Ky \quad (11)$$

where $Kx$ is the sum of the ranks allocated to the first group and $Ky$ is the sum of the ranks awarded to the second group, and $mx$ and $my$ are the number of observations or participants in the first and second groups, respectively. [39] [40]

## 5. Classification

Using LS-SVM, two subject categories, belonging to the Healthy and MDD classes, are defined. LS-SVM is compared with several machine learning methods, including the SVM, KNN, DT, and RF. The 10-fold cross-validation and many assessment metrics, including accuracy, sensitivity, specificity precision, and F-score are used to analyse the classification performance [21].

### 5.1 SVM and LS-SVM

SVM is a potent learning model for classification issues that uses a hyperplane as a decision boundary to divide data points into various categories [20] [19]. The training data is used to create a perfect hyperplane, and the goal of the support vector machine technique is to optimize the distance between the hyperplane and the nearest data points in each group in an N-dimensional space. The ideal model that is produced is then utilized to classify the test data. Let's assume that the given optimization issue can be solved using the provided training dataset $[x_n, y_n]$, as shown below, where the number of samples is represented by $n = 1,2,3 \ldots N$, is and $x_n \in R_n \; and \; y \in (1,-1) \; N$.

The LS-SVM is simply an improved SVM. Kernel mapping and marginal maximization serve as the foundation for LS-SVM model creation [41] [42]. The method used to solve an optimization problem is where the SVM and LS-SVM diverge most. The LS-SVM solves it in a linear manner, while the SVM solves it in a quadratic manner. The LS-SVM is represented mathematically as [41]:

$$E(n) = sign \left[\sum_{n=1}^{N} \alpha_n x_n k(\theta, \theta_n) + b\right] \quad (12)$$

Where $x_n$ = Input data; $\theta_n$=class labels; $\alpha_n$= Lagrangian multiplier; $k(\theta, \theta_n)$=kernel function and $b$=bias [41].

### 5.2 KNN

The k-nearest neighbour approach which, uses training data and a specified k value, searches for the k nearest pieces of information based on distance. If k data have various classes, the algorithm can detect that the category of the unlabelled data will be the exact same as the majority category [43].

### 5.3 DT

Decision Tree is a flowchart that looks like a tree [44]. A test node on a feature corresponds to each internal node. A class label is represented by each leaf node. The branch of the tree represents the test's outcome. The categorization rule is represented by the route from the route node to the leaf node. The most significant feature that is most effective in classifying the tuples is chosen using attributes selection metrics such gini index, gain ratio, and information gain.

**6. Validation**

The suggested method's classification performance in the current study was fairly assessed using 10-fold cross-validation. Using this technique, the dataset is initially divided into 10 folds, of which 9 folds are randomly used as a training set and the 10th fold as a testing set. This procedure is repeated ten times [45] until each fold is used as a testing set. Each cycle results in the application of the trained model to the testing set, producing 10 different evaluation metric values. The various measures employed are described as follows:

$$\text{Accuracy(ACC)} = \frac{\text{TP} + \text{TN}}{\text{TP} + \text{TN} + \text{FP} + \text{FN}} \tag{13}$$

$$\text{Sensitivity(SEN)} = \frac{\text{TP}}{\text{TP} + \text{FN}} \tag{14}$$

$$\text{Specificity(SPE)} = \frac{\text{TN}}{\text{TN} + \text{FP}} \tag{15}$$

$$\text{Precision(Prec)} = \frac{\text{TP}}{\text{TP} + \text{FP}} \tag{16}$$

$$\text{F} - \text{score} = 2 \times \frac{\text{Prec} \times \text{SEN}}{\text{Prec} + \text{SEN}} \tag{17}$$

Where TP represents the overall number of correctly classified MDD samples, FN represents the overall number of MDD samples that were incorrectly classified as HC samples, FP represents the overall number of HC samples that were correctly classified as MDD cases, and TN represents the overall number of correctly classified HC cases [21].

**Results**

The effectiveness of the suggested machine learning method to diagnose MDD based on the EEG signals is assessed in this section in a number of different ways. In the first part, the p-value was used to evaluate these attributes that were taken from all bands. Next, discuss the classification results of all frequency bands and the variance in these bands between participants with MDD and HC. All of the results were performed by taking the EEG signals recorded from 19 channels for all participants.

**1- Results based on features**

The suggested model was tested using the Mann-Whitney U test to eliminate redundant features, and the most significant features were chosen to distinguish healthy patients from those with MDD. These tests determined that the features were approved when their statistic values were 0.05 or less. However, the features with statistical values above 0.05 were rejected as non-significant. Table 2 summarizes the findings of the analysis of the features. Where ApEn, DisEn, shannonEn, and SODP, features were calculated from each frequency band mentioned in Table 1. Shannon entropy and SODP had the smallest p-values, according to the Mann-Whitney U test results for each band.

**Table 2:** The p-value of features extracted from each band.

| | Mann-Whitney U test | | | | |
|---|---|---|---|---|---|
| Features | Delta | Theta | Alpha | Beta | Gamma |
| ApEn | 0.92828 | 0.1096 | 0.30302 | 0.00001 | 0.1096 |
| DisEn | 0.1141 | 0.14986 | 0.11876 | 0.00001 | 0.15854 |
| shannonEn | 0.00001 | 0.00096 | 0.0083 | 0.00048 | 0.14986 |
| SODP | 0.1096 | 0.04136 | 0.87288 | 0.00068 | 0.00001 |

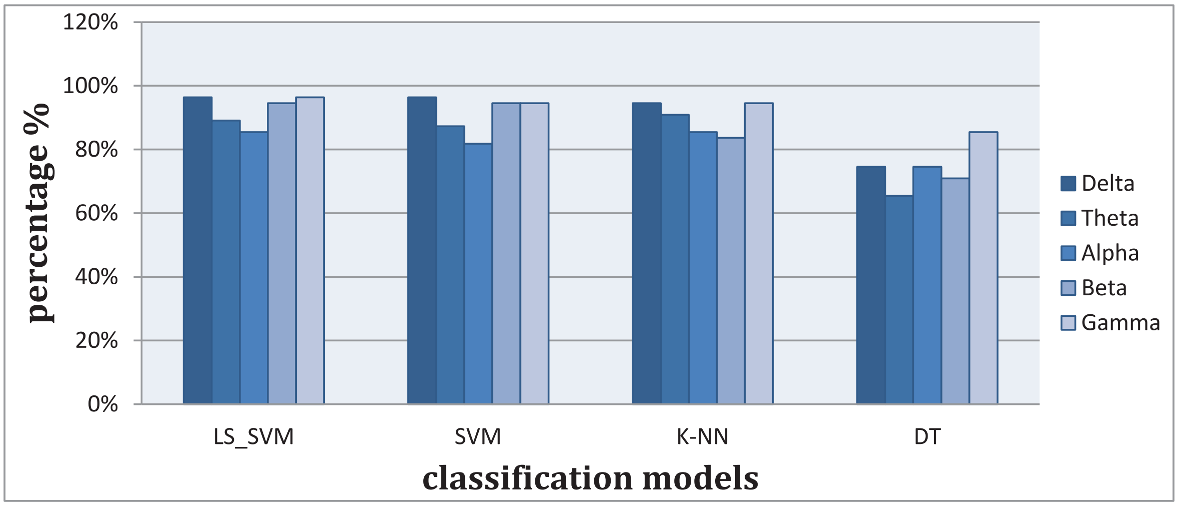


**Figure 3:** Accuracy of (LS-SVM, SVM, KNN, DT) classifiers in all five frequency bands.

**Table 3**: The performance of classification results for the Delta band and all frequency bands.

| | All band | | | | | Delta | | | | |
|---|---|---|---|---|---|---|---|---|---|---|
| classifiers | Acc | Sen | Spe | Pre | F-score | Acc | Sen | Spe | Pre | F-score |
| LS_SVM | 0.9636 | 0.9667 | 0.9600 | 0.9667 | 0.9667 | 0.9636 | 0.9667 | 0.9600 | 0.9667 | 0.9667 |
| SVM | 0.9455 | 0.9333 | 0.9600 | 0.9655 | 0.9492 | 0.9636 | 0.9667 | 0.9600 | 0.9667 | 0.9667 |
| K-NN | 0.9100 | 0.9592 | 0.8627 | 0.8704 | 0.9126 | 0.9455 | 0.9000 | 1 | 1 | 0.9474 |
| DT | 0.7818 | 0.7333 | 0.8400 | 0.8462 | 0.7857 | 0.7455 | 0.7333 | 0.7600 | 0.7857 | 0.7586 |

**Table 4**: The performance of classification results for the Theta band and Alpha.

| | Theta | | | | | Alpha | | | | |
|---|---|---|---|---|---|---|---|---|---|---|
| classifiers | Acc | Sen | Spe | Pre | F-score | Acc | Sen | Spe | Pre | F-score |
| LS_SVM | 0.8909 | 0.8333 | 0.9600 | 0.9615 | 0.8929 | 0.8545 | 0.8000 | 0.9200 | 0.9231 | 0.8571 |
| SVM | 0.8727 | 0.8000 | 0.9600 | 0.9600 | 0.8727 | 0.8182 | 0.7333 | 0.9200 | 0.9167 | 0.8148 |
| K-NN | 0.9091 | 0.8667 | 0.9600 | 0.9630 | 0.9123 | 0.8545 | 0.8667 | 0.8400 | 0.8667 | 0.8667 |
| DT | 0.6545 | 0.4667 | 0.8800 | 0.8235 | 0.5957 | 0.7455 | 0.6667 | 0.8400 | 0.8333 | 0.7407 |

**Table 5:** The performance of classification results for the Beta band and Gamma.

| | Beta | | | | | Gamma | | | | |
|---|---|---|---|---|---|---|---|---|---|---|
| classifiers | Acc | Sen | Spe | Pre | F-score | Acc | Sen | Spe | Pre | F-score |
| LS_SVM | 0.9455 | 0.9000 | 1 | 1 | 0.9474 | 0.9636 | 0.9333 | 1 | 1 | 0.9655 |
| SVM | 0.9455 | 0.9000 | 1 | 1 | 0.9474 | 0.9455 | 0.9667 | 0.9200 | 0.9355 | 0.9508 |
| K-NN | 0.8364 | 0.9667 | 0.6800 | 0.7838 | 0.8657 | 0.9455 | 0.9333 | 0.9600 | 0.9655 | 0.9492 |
| DT | 0.7091 | 0.6000 | 0.8400 | 0.8182 | 0.6923 | 0.8545 | 0.8667 | 0.8400 | 0.8667 | 0.8667 |

**2- Results based on the different frequency bands**

This section presents the results of the classification of each frequency band using the features that were selected by statistical methods (Shannon entropy and SODP). From Tables 3, 4, and 5, we can see the highest performance obtained was from all ranges together using the LS-SVM classifier, where the accuracy = 0.9636, sensitivity = 0.9667, Specificity = 0.9600, Precision= 0.9667, and F-score= 0.9667. As for the performance of each band individually, the highest performance with the LS-SVM classifier was achieved by the Delta band, which achieved accuracy = 0.9636, sensitivity = 0.9667, Specificity = 0.9600, Precision= 0.9667, F-score= 0.9667 and Gamma band which achieved accuracy = 0.9636, sensitivity =0.9333, Specificity = 1, Precision= 1, F-score= 0.9655. In general, the results show that LS-SVM and SVM classifiers perform well across different frequency bands, with high accuracy, sensitivity, specificity, precision, and F-score. K-NN also shows good performance in some cases but with lower specificity. Decision tree (DT) classifier generally performs worse than the other classifiers. When comparing the results across different frequency bands, it can be seen that the performance varies depending on the band. For example, the LS-SVM classifier performs well in the Delta and Beta bands but not as well in the Theta band. Similarly, the K-NN classifier performs well in the Delta band but not as well in the other bands. For a clearer view of the performance of each classifier and all bands, Fig. 3 shows the performance of each classifier in each band.

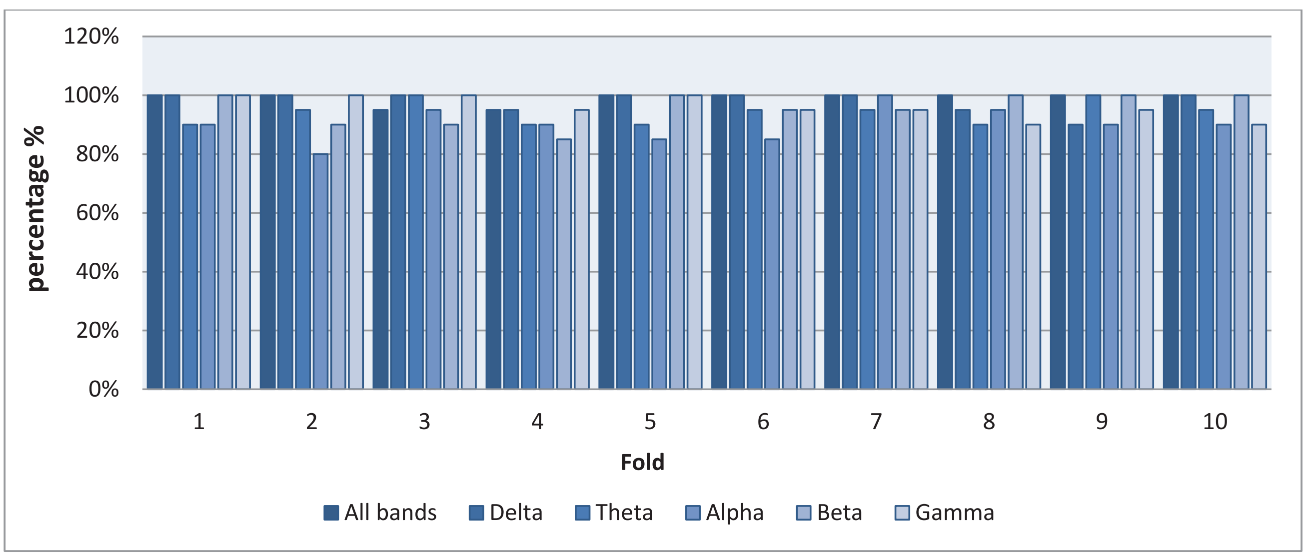


**Figure 4:** The 10-fold cross-validation accuracy of all bands

**Discussion**

The key improvement of the proposed model over prior studies is incorporating nonlinear and SODP features, which were extracted following EEG signal analysis using the Fast-Fourier Transform band filter (FFT band filter). The Mann-Whitney U test was the statistical measure used to evaluate the features. Our results demonstrated that integrating Shannon Entropy with SODP yields a good classification performance. It is notable that a variety of classification models were used in this study and the outcomes revealed that the LS-SVM classifier outperformed the others. The classification results were also verified using 10-cross validation, Fig. 4 reports the classification results based on the 10-cross validation strategy. It can notice that the proposed model obtained a consistent accuracy and there was not a high fluctuation in the results across subjects.

**Conclusions**

In this study, we evaluated samples from 64 participants (30 normal and 34 depressed). Each EEG signal was split into five frequency bands using an FFT band filter. Four features, including approximate entropy, dispersion entropy, Shannon entropy, and SODP features, were then retrieved. Before classifying these features, their effectiveness was examined using statistical metrics. On the open MDD dataset, 10-fold cross-validation w carried out. The experimental findings showed that a high classification rate could be achieved by combining SODP characteristics with Shannon entropy. Also, according to the results of classification, delta and gamma band powers showed the best accuracy also it showed more responsiveness to the existing feature set comparison with other bands, including beta, theta, and alpha. Additionally, the LS-SVM outperformed well-known classification algorithms in terms of performance.

**REFERENCES**

[ 1] **Jaworska, Natalia, et al**. "*Leveraging machine learning approaches for predicting antidepressant treatment response using electroencephalography (EEG) and clinical data*." Frontiers in psychiatry 9 (2019): 768.

[ 2] **Mumtaz, Wajid, et al.** "*A wavelet-based technique to predict treatment outcome for major depressive disorder.*" PloS one 12.2 (2017): e0171409.

[ 3] **Zhu, Jing, et al.** "*Toward depression recognition using EEG and eye tracking: an ensemble classification model CBEM." 2019 IEEE International Conference on Bioinformatics and Biomedicine (BIBM)*. IEEE, 2019.

[ 4] **Jiang, Chao, et al.** "*Enhancing EEG-based classification of depression patients using spatial information.*" IEEE Transactions on Neural Systems and Rehabilitation Engineering 29 (2021): 566-575.

[ 5] **Zhang, Bingtao, et al**. "*Brain functional networks based on resting-state EEG data for major depressive disorder analysis and classification*." IEEE Transactions on Neural Systems and Rehabilitation Engineering 29 (2020): 215-229.

[ 6] **Zhu, Yibo**, et al. "*Classifying major depressive disorder using fNIRS during motor rehabilitation.*" IEEE Transactions on Neural Systems and Rehabilitation Engineering 28.4 (2020): 961-969.

[ 7] **Song, XinWang, et al.** "*LSDD-EEGNet: An efficient end-to-end framework for EEG-based depression detection.*" Biomedical Signal Processing and Control 75 (2022): 103612.

[ 8] **Dev, Antora, et al.** "*Exploration of EEG-based depression biomarkers identification techniques and their applications: A systematic review*." IEEE Access (2022).

[ 9] **Zhu, Yibo, et al.** "*Classifying major depressive disorder using fNIRS during motor rehabilitation.*" *IEEE Transactions on Neural Systems and Rehabilitation Engineering* 28.4 (2020): 961-969.

[ 10] **Dessai, Sukanya, and Soniya Shakil Usgaonkar**. "*Depression Detection on Social Media Using Text Mining.*" *2022 3rd International Conference for Emerging Technology (INCET)*. IEEE, 2022.

[ 11] **Movahed, Reza Akbari, et al.** "*A major depressive disorder classification framework based on EEG signals using statistical, spectral, wavelet, functional connectivity, and nonlinear analysis.*" Journal of Neuroscience Methods 358 (2021): 109209.

[ 12] **Mahato, Shalini, and Sanchita Paul**. "*Detection of major depressive disorder using linear and non-linear features from EEG signals.*" Microsystem Technologies 25.3 (2019): 1065-1076.

[ 13] **Jiang, Chao, et al.** "*Enhancing EEG-based classification of depression patients using spatial information.*" *IEEE transactions on neural systems and rehabilitation engineering* 29 (2021): 566-575.

[ 14] **Harati, Sahar, et al.** "*Depression severity classification from speech emotion.*" *2018 40th Annual International Conference of the IEEE Engineering in Medicine and Biology Society (EMBC)*. IEEE, 2018.

[ 15] **Jiang, Zifan, et al.** "*Classifying major depressive disorder and response to deep brain stimulation over time by analyzing facial expressions*." IEEE Transactions on Biomedical Engineering 68.2 (2020): 664-672.

[ 16] **Acharya, U. Rajendra, et al.** "*A novel depression diagnosis index using nonlinear features in EEG signals.*" European neurology 74.1-2 (2015): 79-83.

[ 17] **Li, Xiaowei, et al.** "*A deep learning approach for mild depression recognition based on functional connectivity using electroencephalography."* Frontiers in neuroscience 14 (2020): 192.

[ 18] **Bachmann, Maie, et al.** "*Methods for classifying depression in single channel EEG using linear and nonlinear signal analysis."* Computer methods and programs in biomedicine 155 (2018): 11-17.

[ 19] **Sharma, Manish, et al**. "*An automated diagnosis of depression using three-channel bandwidth-duration localized wavelet filter bank with EEG signals.*" Cognitive Systems Research 52 (2018): 508-520.

[ 20] **Saeedi, Maryam, Abdolkarim Saeedi, and Arash Maghsoudi.** "*Major depressive disorder assessment via enhanced k-nearest neighbor method and EEG signals*." Physical and Engineering Sciences in Medicine 43.3 (2020): 1007-1018.

[ 21] **Mahato, Shalini, and Sanchita Paul.** "*Classification of depression patients and normal subjects based on electroencephalogram (EEG) signal using alpha power and theta asymmetry*." Journal of medical systems 44.1 (2020): 1-8.

[ 22] **Akbari, Hesam, et al.** "*Depression recognition based on the reconstruction of phase space of EEG signals and geometrical features.*" Applied Acoustics 179 (2021): 108078.

[ 23] **Hagemann, Dirk, Ewald Naumann, and Julian F. Thayer**. "*The quest for the EEG reference revisited: A glance from brain asymmetry research.*" Psychophysiology 38.5 (2001): 847-857.

[ 24] **Teplan, Michal**. "*Fundamentals of EEG measurement*." Measurement science review 2.2 (2002): 1-11.

[ 25] **Newson, Jennifer J., and Tara C. Thiagarajan**. "*EEG frequency bands in psychiatric disorders: a review of resting state studies.*" Frontiers in human neuroscience 12 (2019): 521.

[ 26] **Brigham, E. Oran**. *The fast Fourier transform and its applications*. Prentice-Hall, Inc., 1988.

[ 27] **Almuhammadi, Wafaa S., Khald AI Aboalayon, and Miad Faezipour.** "*Efficient obstructive sleep apnea classification based on EEG signals.*" 2015 Long Island Systems, Applications and Technology. IEEE, 2015.

[ 28] **Shakshi, Ramavtar Jaswal**. "*Brain wave classification and feature extraction of EEG signal by using FFT on lab view.*" Int. Res. J. Eng. Technol 3 (2016): 1208-1212.

[ 29] **Barahona-Pereira, David**. "*Evaluation of feature extraction techniques for an Internet of Things Electroencephalogram.*" (2016).

[ 30] **Bekele, A. J. A. A**. "*Cooley-tukey fft algorithms*." Advanced algorithms (2016).

[ 31] **Vetterling, William T., et al.** Numerical recipes: example book C. Cambridge University Press, 1992.

[ 32] **Delgado-Bonal, Alfonso, and Alexander Marshak.** "*Approximate entropy and sample entropy: A comprehensive tutorial*." Entropy 21.6 (2019): 541.

[ 33] **Wu, Yue, et al.** "*Local Shannon entropy measure with statistical tests for image randomness.*" Information Sciences 222 (2013): 323-342.

[ 34] **Fazan, Frederico Sassoli, et al.** "*Changes in the complexity of heart rate variability with exercise training measured by multiscale entropy-based measurements*." Entropy 20.1 (2018): 47.

[ 35] **Azami, Hamed, and Javier Escudero.** "*Amplitude-and fluctuation-based dispersion entropy.*" Entropy 20.3 (2018): 210.

[ 36] **Akbari, Hesam, et al.** "*Depression Detection Based on Geometrical Features Extracted from SODP Shape of EEG Signals and Binary PSO*." Traitement du Signal 38.1 (2021).

[ 37] **Akbari, Hesam, Sedigheh Ghofrani, and S. Ghofrani.** "*Fast and accurate classification F and NF EEG by using SODP and EWT*." Int J Image Graph Signal Process 11.11 (2019): 29-35.

[ 38] **Singh, Ardra, and A. Amalin Prince**. "*FPGA implementation of second-order difference plot for epileptic seizure detection in EEG signals*." 2015 Annual IEEE India Conference (INDICON). IEEE, 2015.

[ 39] **Nachar, Nadim.** "*The Mann-Whitney U: A test for assessing whether two independent samples come from the same distribution*." Tutorials in quantitative Methods for Psychology 4.1 (2008): 13-20.

[ 40] **Elgendi, Mohamed, et al.** "*Optimization of EEG frequency bands for improved diagnosis of Alzheimer disease.*" 2011 Annual International Conference of the IEEE Engineering in Medicine and Biology Society. IEEE, 2011.

[ 41] **Salankar, Nilima, et al.** "*EEG based alcoholism detection by oscillatory modes decomposition second order difference plots and machine learning*." Biocybernetics and Biomedical Engineering 42.1 (2022): 173-186.

[ 42] **Deng, Wu, et al.** "*A novel intelligent diagnosis method using optimal LS-SVM with improved PSO algorithm.*" Soft Computing 23.7 (2019): 2445-2462.

[ 43] **Chomboon, Kittipong, et al.** "*An empirical study of distance metrics for k-nearest neighbor algorithm.*" Proceedings of the 3rd international conference on industrial application engineering. 2015.

[ 44] **Freund, Yoav, and Llew Mason.** "*The alternating decision tree learning algorithm.*" icml. Vol. 99. 1999.

**Dev, Antora, et al.** "*Exploration of EEG-based depression biomarkers identification techniques and their applications: A systematic review*." *IEEE Acce*